



In the present work, a scenario is introduced in order to explain the magnetic behavior in Central Compact Objects (CCOs). Based on magnetohydrodynamic (MHD) simulations of the post core-collapse supernova phase during the hypercritical accretion episode, we argue that the magnetic field of pulsar could have been early buried. During this phase, thermal neutrinos are created mainly by the pair annihilation, plasmon decay, photo-neutrino emission and other processes. We study the dynamics of these neutrinos in this environment and then, we estimate the number and the flavor ratio of neutrinos expected on Earth. The neutrino burst is the only viable observable that could provide compelling evidence of the hypercritical phase and then, the hidden magnetic field scenario as an alternative one that could explain the anomalous low magnetic fields estimated for CCOs.



Currently there are nine confirmed CCOs (Luo et al. 2015) with similar common features (see Table 1):

- The location of these compact objects has been found near the center of some young supernova remnants (SNRs).
- A counterpart emission detected in optical or radio wavelengths.
- The non detection of pulsar wind nebulae from these sources.
- The thermal spectrum observed in the soft X-ray band (peaking at $kT_{BB} \sim 0.2 - 0.6$ keV) with high luminosities $L_X \sim 10^{33} - 10^{34}$ erg s⁻¹ (de Luca 2008).

CCO	SNR	d (kpc)	B (G)	t (kyr)	L_x erg s ⁻¹
XMMU J173203.3-344518	G 353.6-0.7	3.2	$(1 - 10) \times 10^{11}$	27	1.1×10^{33}
CXOU J232327.9+584842	Cas A	3.4	$(1 - 5) \times 10^{11}$	0.33	4.7×10^{33}
CXOU J185238+0040020	Kes 79	7	3.1×10^{10}	7	5.3×10^{33}
RX J0822.0-4300	Puppis A	2.2	2.9×10^{10}	4.5	5.6×10^{33}
1E 1207.4-5209	PKS 1209-51/52	2.1	9.8×10^{10}	7	2.5×10^{33}
CXOU J160103-513353	G330.2+1.0	4.9	$(0, 1, 10) \times 10^{12}$	3.3	1.5×10^{33}
1WGA J1713.4-3949	G347.3-0.5	1.3		1.6	3.74×10^{33}
XMMU J172054.5-372652	G350.1-0.3	9.0		0.9	3.9×10^{33}
CXOU J085201.4-461753	G266.1-1.2	0.33		1	2.5×10^{33}

Table 1. Observable quantities of the confirmed CCOs (Gotthelf 2013).

During a core-collapse supernova the high strength of magnetic field is submerged by the hypercritical accretion (Muslimov & Page 1995). The conditions needed for the formation of a neutron star (NS) inside supernovae are convective envelope, hyperaccretion of material and submergence of the magnetic field on the stellar crust.

Using these conditions, simple 1D ideal MHD simulation were performed to show that hypercritical accretion is related with the submergence of the magnetic field (Geppert et al. 1999). This simulation showed a prompt submergence of magnetic field lines into the NS.

In the hypercritical accretion phase, thermal neutrinos are generated by several processes. These neutrinos will oscillate in accordance with the density of regions I, II, III, IV and in vacuum into Earth (see Table 2). Neutrinos properties are modified when they go through the regions during the hypercritical accretion phase and resonant conversions of neutrino flavors are expected.

Zones	Density (g cm ⁻³)	Radii (cm)	Description
I. New crust of NS surface ($r \leq [r_{ns} + r_c]$)	$\rho_c(T, B)$	$r_{ns} = 10^6$ $r_c \approx 10^{2.5}$	1. A new crust with strong B is formed by hypercritical phase. 2. Magnetic field in the range $10^{11} \leq B \leq 10^{13}$ G could be submerged. 3. Photons and neutrinos confined are thermalized to a few MeV.
II. Quasi-hydrostatic envelope ($[r_{ns} + r_c] \leq r \leq r_s$)	$10^{2.9} (\frac{r}{r_s})^3$	$r_s \approx 10^{8.9}$	1. Reverse shock induces hypercritical accretion onto the new NS surface. 2. A new expansive shock is formed by the material accreted and bounced off. 3. The high pressure close to NS surface allows the e^\pm process to be dominant.
III. Free-fall ($r_s \leq r \leq r_h$)	$10^{-1.24} (\frac{r}{r_h})^{-3/2}$	$r_h = 10^{10.8}$	1. Material begin falling with velocity $\sqrt{\frac{2GM}{4\pi r^2 \sigma(r)}}$ and density $\frac{M}{4\pi r^3 \sigma(r)}$.
IV. External layers ($r_h \leq r$)	$10^{-5.2} A (\frac{R_* - 1}{k})^k$ $(k, A) = \begin{cases} (2.1, 20); & r_h < r < r_a, \\ (2.5, 1); & r > r_a. \end{cases}$	$R_* \approx 10^{12.5}$ $r_a = 10^{11}$	1. The typical profile of the external layers is presented.

Table 2. Densities and radii of the zones evolved in the hypercritical accretion episode.

In this work, we use the FLASH code in order to simulate i) the hyper-accretion phase onto the newborn NSs, focusing on the dynamics and morphology of magnetized and thermal plasma, ii) the magnetic field evolution through magnetic reconnections into stellar surface and iii) the neutrino luminosity for the known CCOs. In addition, the thermal neutrino flux and the flavor ratio expected on Earth are computed.

Figure 1 shows a schematic diagram of the reverse shock, the formation of a quasi-hydrostatic envelope and the complex dynamics around the newly born compact remnant, including the neutrino cooling processes.

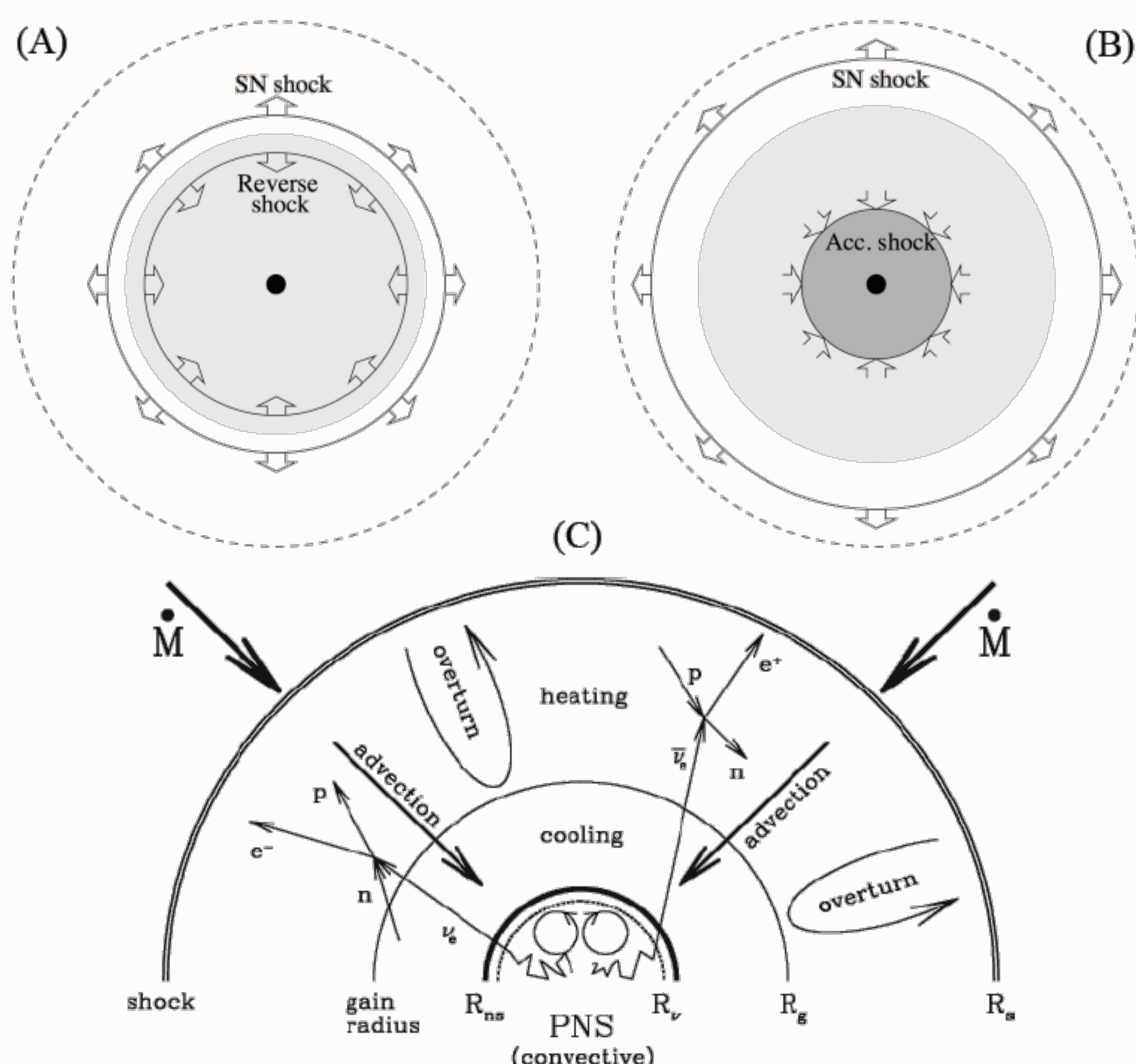


Figure 1. Hypercritical accretion phase schematic diagram. (A) The formation of the reverse shock; (B) The formation of quasi-hydrostatic envelope with an accretion shock and (C) The complex dynamics around the newborn NS during such phase.

Figure 2 shows the temporal evolution of matter density superimposed with the magnetic field contours, and also the magnetic energy density.

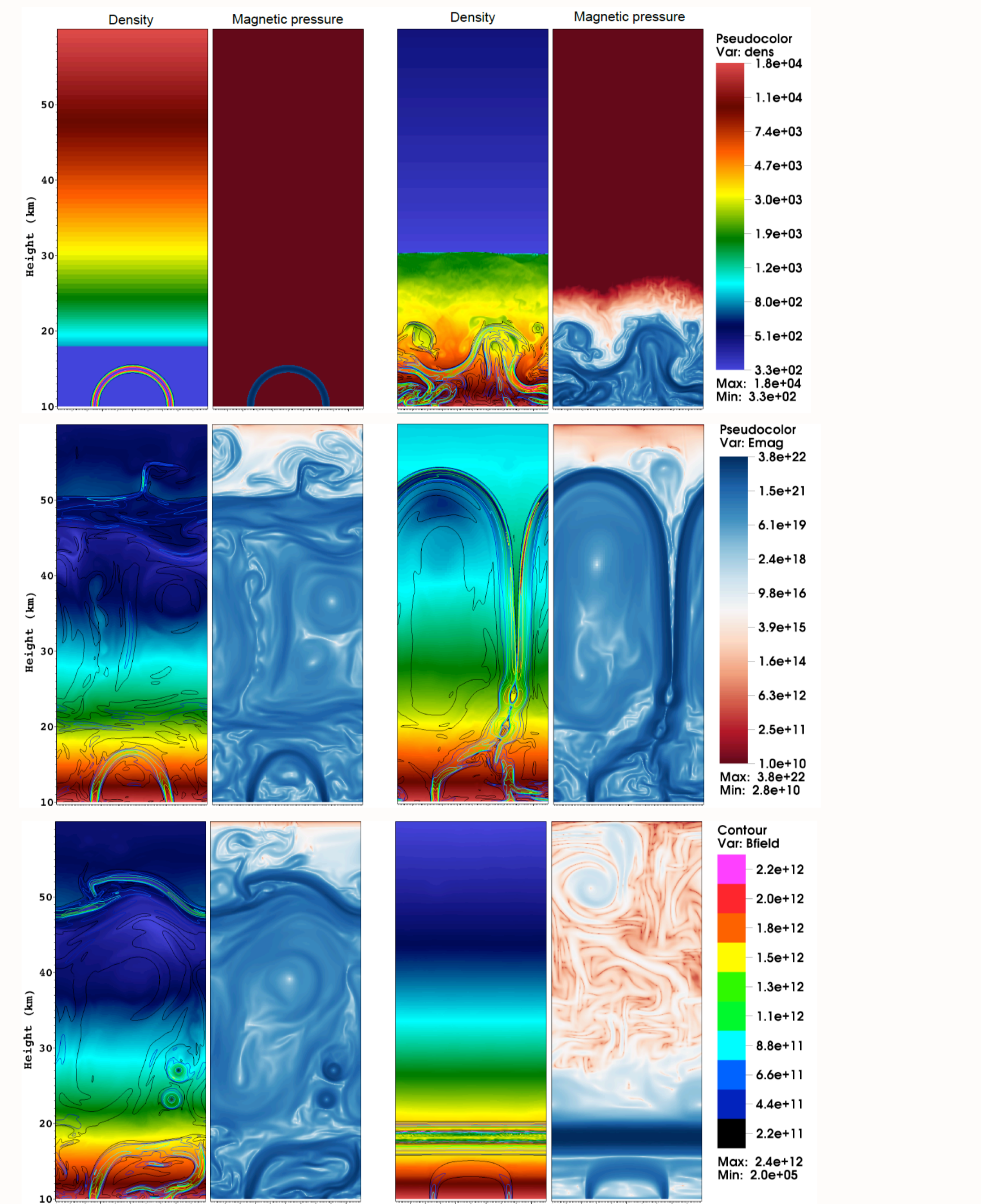


Figure 2. Color maps of density, with magnetic field contours were superimposed, and magnetic energy for the case $h = 0.001m_p$. We show several time-steps of the evolution of the magnetic loop to analyze the magnetic reconnection process. Upper panels: (left: $t = 0$ ms; right: $t = 1$ ms). Middle panels: (left: $t = 20$ ms; right: $t = 100$ ms). Bottom panels: (left: $t = 400$ ms; right: $t = 1000$ ms).

The plasma thermalized at ≈ 4 MeV is submerged in a magnetic field of $\approx 2.6 \times 10^{10}$ G. Regarding the neutrino effective potential in this region, the neutrino effective potential is plotted as a function of temperature and chemical potential in Figure 3. This plot shows the positivity of the effective potential, hence the neutrinos can oscillate resonantly.

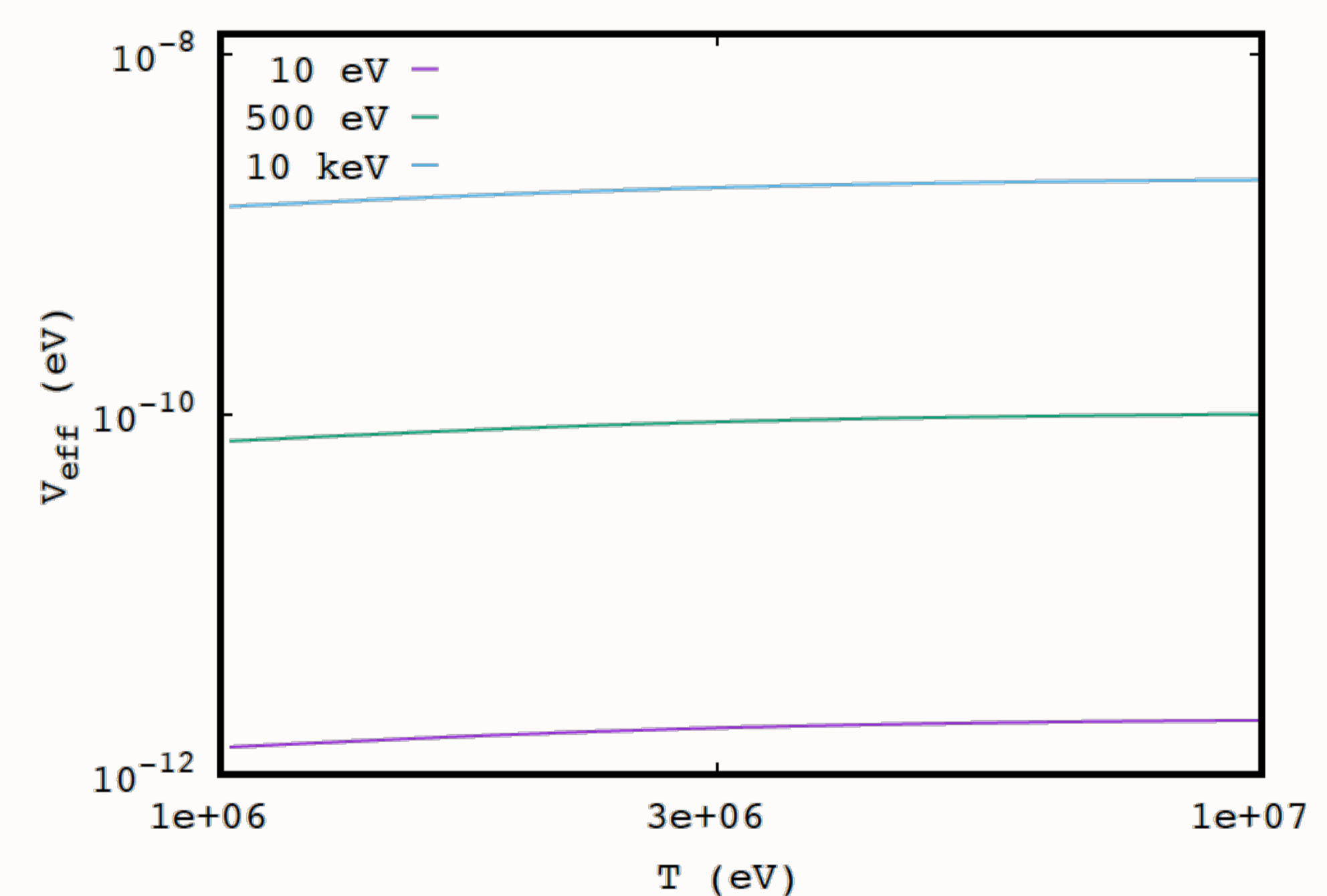


Figure 3. Neutrino effective potential as a function of temperature and chemical potential for a magnetic field of 2.9×10^{10} G.

Neutrinos can oscillate resonantly in regions II, III y IV due to the density profile of the collapsing material surrounding the progenitor. Taking into consideration the oscillation probabilities in each region and in the vacuum, the flavor ratio expected on Earth for neutrino energies of $E_\nu = 1, 5, 10$ and 20 MeV for several CCOs was estimated and shown in Table 3.

E_ν	XMMU J173203.3	1E 1207.4	CXOU J160103	1WGA J1713.4	XMMU J172054.5	CXOU J085201.4
1	1.036:0.988:0.976	1.035:0.989:0.976	1.034:0.988:0.978	1.036:0.987:0.975	1.037:0.987:0.976	1.034:0.989:0.977
5	1.037:0.987:0.975	1.038:0.986:0.975	1.035:0.989:0.975	1.036:0.987:0.976	1.037:0.988:0.974	1.035:0.988:0.976
10	1.040:0.977:0.984	1.041:0.976:0.984	1.042:0.975:0.984	1.039:0.978:0.985	1.040:0.978:0.983	1.041:0.977:0.983
20	1.045:0.933:0.982	1.044:0.934:0.982	1.043:0.934:0.983	1.044:0.933:0.983	1.046:0.932:0.982	1.043:0.934:0.983

Table 3. The neutrino flavor ratio expected on Earth with $E_\nu = 1, 5, 10$ and 20 MeV for several CCOs.

References

- De Luca, A., Bassa, C., Wang, Z., Cumming, A., & Kaspi, V., 2008in, AIP, 311-319
 Fraija, N., 2014, MNRAS, 437, 2187
 Geppert, U., Page, D., & Zannias, T., 1999, A&A, 345, 847
 Gotthelf, E. V., Halpern, J. P., & Alford, J., 2013, ApJ, 765, 58
 Luo, J., Ng, C., Ho., W., et al., 2015, ApJ, 808, 130
 Muslimov, A., & Page, D., 1995, ApJ, 440 L77

Acknowledgements

We thank CONACyT scholarship (825482) and UNAM-DGAPA-PAPIIT through grant IA102917 for financial support. The software used in this work was partially developed by the DOE NNSA-ASC OASCR FLASH Center at the University of Chicago.